Biomedical Optics EXPRESS

Lymphatic abnormalities in the normal contralateral arms of subjects with breast cancer-related lymphedema as assessed by near-infrared fluorescent imaging

Melissa B. Aldrich,[1] Renie Guilliod,[2] Caroline E. Fife,[2] Erik A. Maus,[2] Latisha Smith,[2] John C. Rasmussen,[1] and Eva M. Sevick-Muraca[1,*]

[1]*Center for Molecular Imaging, The Brown Foundation Institute for Molecular Medicine, University of Texas Health Science Center-Houston, 1825 Pressler, 330A, Houston, TX 77030, USA*
[2]*Memorial Hermann Center for Wound Healing, Memorial Hermann Hospital, 6411 Fannin Street, Houston, TX 77030, USA*
**Eva.Sevick@uth.tmc.edu*

Abstract: Current treatment of unilateral breast cancer-related lymphedema (BCRL) is only directed to the afflicted arm. Near-infrared fluorescent imaging (NIRF) of arm lymphatic vessel architecture and function in BCRL and control subjects revealed a trend of increased lymphatic abnormalities in both the afflicted and unafflicted arms with increasing time after lymphedema onset. These pilot results show that BCRL may progress to affect the clinically "normal" arm, and suggest that cancer-related lymphedema may become a systemic, rather than local, malady. These findings support further study to understand the etiology of cancer-related lymphedema and lead to better diagnostics and therapeutics directed to the systemic lymphatic system.

OCIS codes: (110.0110) Imaging systems; (170.3880) Medical and biological imaging; (230.0230) Optical devices.

References and links

1. K. Sato, "Current technical overviews of sentinel lymph node biopsy for breast cancer," Breast Cancer **14**(4), 354–361 (2007).
2. J. M. Armer and B. R. Stewart, "Post-breast cancer lymphedema: incidence increases from 12 to 30 to 60 months," Lymphology **43**(3), 118–127 (2010).
3. Y. Ohba, Y. Todo, N. Kobayashi, M. Kaneuchi, H. Watari, M. Takeda, S. Sudo, M. Kudo, H. Kato, and N. Sakuragi, "Risk factors for lower-limb lymphedema after surgery for cervical cancer," Int. J. Clin. Oncol. **16**(3), 238–243 (2011).
4. J. N. Cormier, R. L. Askew, K. S. Mungovan, Y. Xing, M. I. Ross, and J. M. Armer, "Lymphedema beyond breast cancer: a systematic review and meta-analysis of cancer-related secondary lymphedema," Cancer **116**(22), 5138–5149 (2010).
5. J. E. Zuther, *Lymphedema Management: the Comprehensive Guide for Practitioners* (Thieme Medical, New York, 2005).
6. C. Kunos, F. Simpkins, H. Gibbons, C. Tian, and H. Homesley, "Radiation therapy compared with pelvic node resection for node-positive vulvar cancer: a randomized controlled trial," Obstet. Gynecol. **114**(3), 537–546 (2009).
7. C. P. Allan, A. J. Hayes, and J. M. Thomas, "Ilioinguinal lymph node dissection for palpable metastatic melanoma to the groin," ANZ J. Surg. **78**(11), 982–986 (2008).
8. H. Tada, S. Teramukai, M. Fukushima, and H. Sasaki, "Risk factors for lower limb lymphedema after lymph node dissection in patients with ovarian and uterine carcinoma," BMC Cancer **9**(1), 47 (2009).
9. A. J. Spillane, R. P. Saw, M. Tucker, K. Byth, and J. F. Thompson, "Defining lower limb lymphedema after inguinal or ilio-inguinal dissection in patients with melanoma using classification and regression tree analysis," Ann. Surg. **248**(2), 286–293 (2008).
10. S. B. Chang, R. L. Askew, Y. Xing, S. Weaver, J. E. Gershenwald, J. E. Lee, R. Royal, A. Lucci, M. I. Ross, and J. N. Cormier, "Prospective assessment of postoperative complications and associated costs following inguinal lymph node dissection (ILND) in melanoma patients," Ann. Surg. Oncol. **17**(10), 2764–2772 (2010).

#167423 - $15.00 USD Received 3 March 2012; revised 27 Apr 2012; accepted 27 Apr 2012; published 3 May 2012

11. K. May, A. Bryant, H. O. Dickinson, S. Kehoe, and J. Morrison, "Lymphadenectomy for the management of endometrial cancer," Cochrane Database of Systematic Reviews 2010, Issue 1, Art. No. CD007585, Jan. 20, 2010.
12. P. Klernäs, L. J. Kristjanson, and K. Johansson, "Assessment of quality of life in lymphedema patients: validity and reliability of the Swedish version of the Lymphedema Quality of Life Inventory (LQOLI)," Lymphology **43**(3), 135–145 (2010).
13. E. U. Cidón, C. Perea, and F. López-Lara, "Life after breast cancer: dealing with lymphoedema," Clin Med Insights Oncol **5**, 9–14 (2011).
14. M. Stamatakos, C. Stefanaki, and K. Kontzoglou, "Lymphedema and breast cancer: a review of the literature," Breast Cancer **18**(3), 174–180 (2011).
15. D. S. Ko, R. Lerner, G. Klose, and A. B. Cosimi, "Effective treatment of lymphedema of the extremities," Arch. Surg. **133**(4), 452–458 (1998).
16. R. Sharma, J. A. Wendt, J. C. Rasmussen, K. E. Adams, M. V. Marshall, and E. M. Sevick-Muraca, "New horizons for imaging lymphatic function," Ann. N. Y. Acad. Sci. **1131**(1), 13–36 (2008).
17. J. C. Rasmussen, I.-C. Tan, M. V. Marshall, C. E. Fife, and E. M. Sevick-Muraca, "Lymphatic imaging in humans with near-infrared fluorescence," Curr. Opin. Biotechnol. **20**(1), 74–82 (2009).
18. J. C. Rasmussen, I.-C. Tan, M. V. Marshall, K. E. Adams, S. Kwon, C. E. Fife, E. A. Maus, L. A. Smith, K. R. Covington, and E. M. Sevick-Muraca, "Human lymphatic architecture and dynamic transport imaged using near-infrared fluorescence," Transl Oncol **3**(6), 362–372 (2010).
19. K. E. Adams, J. C. Rasmussen, C. Darne, I.-C. Tan, M. B. Aldrich, M. V. Marshall, C. E. Fife, E. A. Maus, L. A. Smith, R. Guilloid, S. Hoy, and E. M. Sevick-Muraca, "Direct evidence of lymphatic function improvement after advanced pneumatic compression device treatment of lymphedema," Biomed. Opt. Express **1**(1), 114–125 (2010).
20. I.-C. Tan, E. A. Maus, J. C. Rasmussen, M. V. Marshall, K. E. Adams, C. E. Fife, L. A. Smith, W. Chan, and E. M. Sevick-Muraca, "Assessment of lymphatic contractile function after manual lymphatic drainage using near-infrared fluorescence imaging," Arch. Phys. Med. Rehabil. **92**(5), 756–764.e1 (2011).
21. E. M. Sevick-Muraca, "Translation of near-infrared fluorescence imaging technologies: emerging clinical applications," Annu. Rev. Med. **63**(1), 217–231 (2012).
22. M. V. Marshall, J. C. Rasmussen, I.-C. Tan, M. B. Aldrich, K. E. Adams, X. Wang, C. E. Fife, E. A. Maus, L. A. Smith, and E. M. Sevick-Muraca, "Near-infrared fluorescence imaging in humans with indocyanine green: a review and update," The Open Surg. Oncol. J. **2**(2), 12–25 (2010).
23. T. Yamamoto, N. Yamamoto, K. Doi, A. Oshima, H. Yoshimatsu, T. Todokoro, F. Ogata, M. Mihara, M. Narushima, T. Iida, and I. Koshima, "Indocyanine green-enhanced lymphography for upper extremity lymphedema: a novel severity staging system using dermal backflow patterns," Plast. Reconstr. Surg. **128**(4), 941–947 (2011).
24. G. Cooper, "Early diagnosis of lymphoedema helps to reduce its psychological and social impact," Nurs. Times **106**(49–50), 15–17 (2010).
25. N. L. Stout Gergich, L. A. Pfalzer, C. McGarvey, B. Springer, L. H. Gerber, and P. Soballe, "Preoperative assessment enables the early diagnosis and successful treatment of lymphedema," Cancer **112**(12), 2809–2819 (2008).
26. L. M. Sena, S. J. Fishman, K. J. Jenkins, H. Xu, M. W. Brechbiel, C. A. Regino, N. Kosaka, M. Bernardo, P. L. Choyke, and H. Kobayashi, "Magnetic resonance lymphangiography with a nano-sized gadolinium-labeled dendrimer in small and large animal models," Nanomedicine (Lond) **5**(8), 1183–1191 (2010).
27. Y. E. Chung, W. J. Hyung, S. Kweon, S. J. Lim, J. Choi, M. H. Lee, H. Kim, S. Myoung, and J. S. Lim, "Feasibility of interstitial CT lymphography using optimized iodized oil emulsion in rats," Invest. Radiol. **45**(3), 142–148 (2010).
28. J. Park, S. Kim, I. G. Jeong, C. Song, J. H. Hong, C. S. Kim, and H. Ahn, "Does the greater number of lymph nodes removed during standard lymph node dissection predict better patient survival following radical cystectomy?" World J. Urol. **29**(4), 443–449 (2011).
29. A. E. Giuliano, K. K. Hunt, K. V. Ballman, P. D. Beitsch, P. W. Whitworth, P. W. Blumencranz, A. M. Leitch, S. Saha, L. M. McCall, and M. Morrow, "Axillary dissection vs no axillary dissection in women with invasive breast cancer and sentinel node metastasis: a randomized clinical trial," JAMA **305**(6), 569–575 (2011).
30. G. H. Sakorafas, G. Peros, L. Cataliotti, and G. Vlastos, "Lymphedema following axillary lymph node dissection for breast cancer," Surg. Oncol. **15**(3), 153–165 (2006).
31. A. Soran, W. C. Wu, A. Dirican, R. Johnson, O. Andacoglu, and J. Wilson, "Estimating the probability of lymphedema after breast cancer surgery," Am. J. Clin. Oncol. **34**(5), 506–510 (2011).
32. S. H. Ridner, M. S. Dietrich, B. R. Stewart, and J. M. Armer, "Body mass index and breast cancer treatment-related lymphedema," Support. Care Cancer **19**(6), 853–857 (2011).
33. M. L. Kwan, J. Darbinian, K. H. Schmitz, R. Citron, P. Partee, S. E. Kutner, and L. H. Kushi, "Risk factors for lymphedema in a prospective breast cancer survivorship study: the Pathways Study," Arch. Surg. **145**(11), 1055–1063 (2010).
34. K. M. Burnand, D. M. Glass, P. S. Mortimer, and A. M. Peters, "Lymphatic dysfunction in the apparently clinically normal contralateral limbs of patients with unilateral lower limb swelling," Clin. Nucl. Med. **37**(1), 9–13 (2012).

#167423 - $15.00 USD Received 3 March 2012; revised 27 Apr 2012; accepted 27 Apr 2012; published 3 May 2012

35. S. J. Pain, R. W. Barber, J. R. Ballinger, C. K. Solanki, P. S. Mortimer, A. D. Purushotham, and A. M. Peters, "Local vascular access of radioprotein injected subcutaneously in healthy subjects and patients with breast cancer-related lymphedema," J. Nucl. Med. **45**(5), 789–796 (2004).
36. S. J. Pain, A. D. Purushotham, R. W. Barber, J. R. Ballinger, C. K. Solanki, P. S. Mortimer, and A. M. Peters, "Variation in lymphatic function may predispose to development of breast cancer-related lymphoedema," Eur. J. Surg. Oncol. **30**(5), 508–514 (2004).
37. S. Modi, A. W. Stanton, W. E. Svensson, A. M. Peters, P. S. Mortimer, and J. R. Levick, "Human lymphatic pumping measured in healthy and lymphoedematous arms by lymphatic congestion lymphoscintigraphy," J. Physiol. **583**(1), 271–285 (2007).
38. S. K. Daley, M. J. Bernas, B. D. Stea, F. Bracamonte, M. McKenna, A. Stejskal, E. D. Hirleman, and M. H. Witte, "Radioprotection from radiation-induced lymphedema without tumor protection," Lymphology **43**(2), 48–58 (2010).

1. Introduction

Axillary lymph node dissection (ALND) has been a part of standard surgical treatment of breast cancer, enabling regional control of the disease and reliable staging based upon the identification of nodal metastases. ALND, however, is also associated with unacceptable surgical morbidities, particularly breast cancer-related lymphedema (BCRL), a disfiguring, debilitating disease that has no cure. Sentinel lymph node dissection (SLND) enables staging from the tumor-draining axillary lymph nodes with reduced risk of morbidity [1], but ALND remains the standard of practice if sentinel lymph nodes (SLNs) are found to contain metastases. While BCRL is less associated with cancer survivors who undergo SLND compared to those who undergo ALND, SLND alone still carries risk for BCRL.

Reports of incidence rates of lymphedema vary widely, but a recent study found that, depending on criteria used, 43% to 94% of all breast cancer survivors developed lymphedema within 60 months post-operatively [2]. It is noteworthy that lymphedema is also prevalent after other cancer surgeries besides ALND and SLND: 20% of cervical cancer survivors [3] and many prostate cancer survivors [4,5] suffer lower-extremity lymphedema. Extended pelvic lymph node dissection (ePLND) in bladder, prostate, and melanoma surgeries is also associated with high incidence rates of lymphedema [6–11].

The etiology of lymphedema is not well understood. Lymph node removal and radiation treatment is thought to impair the normal lymphatic function of transporting excess fluid and macromolecules away from tissues for return to the blood vasculature. When the lymphatic vasculature is impaired, or becomes overwhelmed over time, fluid and macromolecule buildup occurs, leading to irresolvable and progressive swelling. If left untreated, lymphedema is disfiguring, and patients are prone to infections, fibrosis, depression, certain sarcomas, sepsis, and arthritis [12–14]. While some patients respond to treatment regimens of complete decongestive therapy (CDT), which includes manual lymphatic drainage (MLD), compression bandaging, therapeutic exercise, and meticulous skin care, only 59.1% of patients with arm lymphedema respond over a treatment period of 12 months [15].

To date, there has been no accepted method with sufficient spatial resolution to non-invasively image the lymphatics and their function [16]. Recently, we developed a near-infrared fluorescence (NIRF) imaging technique that demonstrated the feasibility of imaging lymphatics in normal controls and persons suffering lymphedema [17,18], as well as lymphatic functional response to MLD and pneumatic compression devices [19,20]. NIRF imaging depends upon the intradermal administration of the fluorescent dye indocyanine green (ICG), which is actively taken up by the initial lymphatics in the dermis and transits to collecting lymphatics through a series of lymphangions, or segments of "pumping" vessels, that conduct lymph to draining lymph node basins. Upon illuminating tissues with dim, tissue-penetrating NIR light, ICG-laden lymph generates fluorescence which is then collected to generate dynamic lymphatic imaging [21]. As part of a larger study, we recently imaged a number of BCRL subjects with a variety of lymphatic anomalies and observed a trend of prevalence in both affected and unaffected arms with time after the initial onset of lymphedema symptoms. This contribution describes collected images, associates time

#167423 - $15.00 USD Received 3 March 2012; revised 27 Apr 2012; accepted 27 Apr 2012; published 3 May 2012

following BCRL onset to the severity and quantity of lymphatic vessel abnormalities in both affected and unaffected limbs, and suggests that cancer related-lymphedema may become a systemic, rather than local, malady.

2. Methods

2.1. Participants/subject population

The protocol used for this study was approved by the U.S. Food and Drug Administration under a combinational investigational new drug application for the off-label use of indocyanine green as a NIRF contrast agent (IND #102,827, NCT00833599, "Imaging lymphatic function in normal subjects and in persons with lymphatic disorders"). The studies were approved by the University of Texas Health Science Center institutional review board. Written informed consent was gathered from all participants—18 BCRL subjects and 6 normal control subjects. The BCRL subjects (age 45–68, 17 women and 1 man) self-reported times since cancer treatment and the onset of BRCL. The NIRF imaging results from BCRL subjects were classified into 3 groups: (i) 6 months or less, (ii) between 1 and 2 years, and (iii) greater than 5 years since self-reported onset of BCRL symptoms. Normal subjects ranged from 26 to 68 years of age, and included 5 women and 1 man.

2.2. Instruments for NIRF imaging

The investigational imaging system depicted in Fig. 1 is described elsewhere [17–22]. Briefly, each system consists of a 785-nm excitation light source, a NIR-sensitive Gen III (model FS9910C) image intensifier, and a customized charge-coupled device (CCD) 16-bit camera outfitted with filters to selectively collect ICG fluorescence at 830 nm. The imaging field of view is determined by the distance of the camera from the subject and ranges from ~15

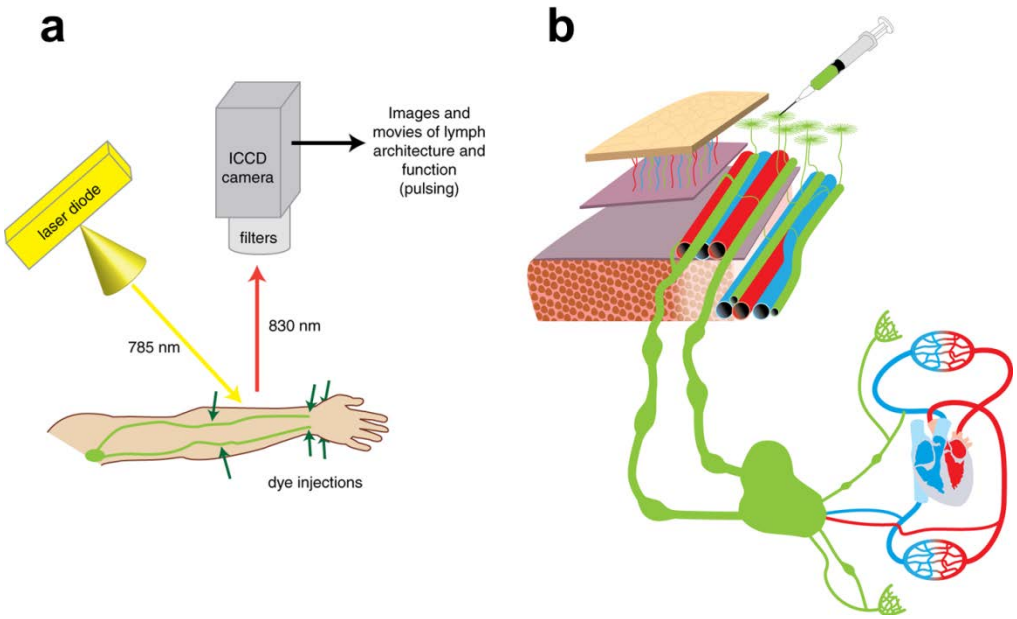

Fig. 1. System used for NIRF lymphatic imaging. (a) Each system consists of a 785-nm excitation light source, a NIR-sensitive image intensifier, and a customized charge-coupled device (CCD) camera outfitted with filters to selectively collect ICG fluorescence at 830 nm. The emitted excitation light covered a maximal tissue surface area of approximately 900 cm^2. Injected ICG typically entered lymphatic capillaries near injection sites, and then moved into pre-collector and collector lymphatic vessels in subject arms. (b) Indocyanine green (ICG) is injected intradermally for uptake by dermal lymphatic capillaries, which feed into lymphatic pre-collector and collector vessels.

#167423 - $15.00 USD Received 3 March 2012; revised 27 Apr 2012; accepted 27 Apr 2012; published 3 May 2012

centimeters to ~61 centimeters. At an imaging distance of ~30 centimeters, the spatial resolution is approximately 1.26 line pairs per millimeter, as determined using the 1951 United States Air Force resolution test chart. Excitation at 785 nanometers was used, because 785 nm laser diodes are readily available, and this wavelength is near the peak excitation of the fluorophore used, indocyanine green (780 nm). The emitted excitation light illuminated a maximal tissue surface area of approximately 900 cm^2, resulting in an incident laser diode power of <1.9 mW/cm^2. An exposure time of 200 milliseconds per image permitted near real-time imaging of the lymphatics. The field of view varies according to distance between camera and subject (6-3 inches), and depths of 3–4 centimeters are routinely imaged.

2.3. Procedures

Twelve injections each of 0.1 cc of 0.25 mg/ml indocyanine green were administered intradermally at the following anatomical locations: two injections dorsally on each hand, two in the medial and lateral ventral sides of each wrist, and two in the upper lateral area of each forearm, for a total dose of 300 micrograms. Injection sites were covered with small round adhesive bandages, and sometimes with black vinyl tape, to prevent camera saturation from intense fluorescence. Immediately following ICG administration, subjects were imaged. The following views were collected: (i) the dorsal hand, (ii) the dorsal forearm, (iii) the ventral forearm, (iv) the medial view of the elbow, and (v) the axilla.

2.4. Analysis

Images were loaded into ImageJ software (NIH) for analysis, and presented as still images or a movie compilation of still images. Images were evaluated for lymphovascular anomalies. For each NIRF image of the lymphatic vessels in hand, forearm, elbow and axilla views, the numbers of abnormalities in affected and unaffected arms of BCRL subjects were assessed by consensus of authors.

3. Results

3.1. Control subjects present with normal lymphatic architecture

Figure 2 provides NIRF images of a single subject that is representative of all normal controls. As shown in Fig. 2(a), typical images of the hand consist of two major lymphatic vessel bundles draining from the injection sites and into the forearm. No distal flow of ICG toward fingers or toward the palms was observed in normal subjects. The dorsal view of the forearms (Fig. 2[b]) typically displayed the delivery of lymph to the upper arm through the lymphatic bundles that drained dorsal injection sites in the hand. Typical drainage patterns associated with medial and lateral wrist injections are seen in the ventral view of the forearm (Fig. 2[c]), along with numerous lymphatic vessels. ICG-laden lymph "packets," presumably within lymphangions, are readily identified, and some brachial lymph nodes are visible. Images of the elbow (Fig. 2[d]) typically displayed numerous lymph vessels in the forearm

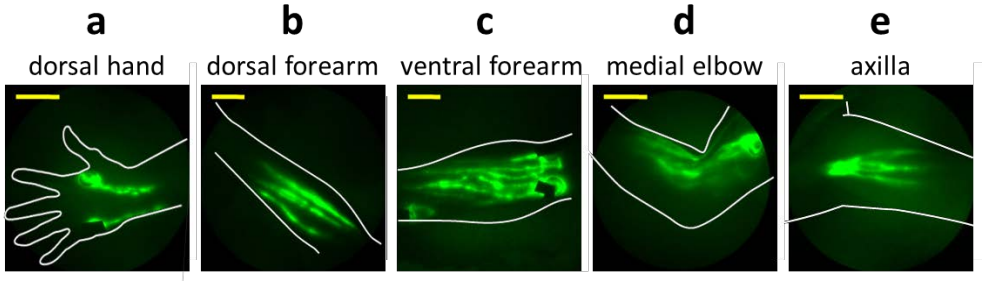

Fig. 2. Near-infrared images of lymphatic vessels in (a) dorsal hand, (b) dorsal forearm, (c) ventral forearm, (d) medial elbow, and (e) axilla of a healthy control subject. Yellow scale bars = 5 cm.

#167423 - $15.00 USD Received 3 March 2012; revised 27 Apr 2012; accepted 27 Apr 2012; published 3 May 2012

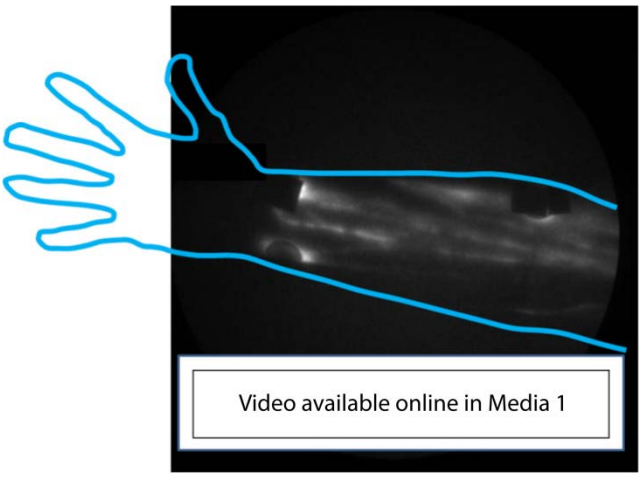

Fig. 3. “Pumping,” or lymphatic propulsion, in a normal healthy control subject arm. Lymph “packets” are visible moving from valve to valve along lymphatic vessels (Media 1). Shown are multiple lymphatic vessels in a normal, healthy control ventral forearm.

and upper arm areas, sometimes with “packets” of ICG-laden lymph collecting at sites of presumed lymphangions before being “pumped” through contractile motions to the next lymphangions (Fig. 3, Media 1). Axilla images were taken while the arm was positioned over the head, and displayed vessels actively pumping ICG-laden lymph to axillary lymph nodes (Fig. 2[e]). In summary, all control subjects exhibited active ICG transport within straight lymphatic vessels and confinement of extravascular ICG to within a 0.5 cm radius of the intradermal injection site.

3.2. Aberrant lymphatic vessel architecture is evident in BCRL subjects

NIRF imaging of lymphedema subjects revealed departures from normal lymphatic vessel architecture in both diagnosed as well as contralateral, unaffected arms. Examples of the lymphatic phenotypes typically seen in BCRL subjects are depicted in Fig. 4. While we and others have noted these distinct phenotypes in patients with lymphedema [17,18,23], we reintroduce them here in the context of our imaging of BCRL as a function of time after onset.

Fine hyperplasia of vessels/tortuous lymphatic bundles (Fig. 4[a], top). In some subjects, small ICG-laden capillary lymphatic vessels were observed in the dermis, far from the site of injection. In some cases these dermal regions filled with ICG-laden lymph *via* conducting lymphatic vessels that could be seen actively pumping lymph. It remains unknown whether these apparently hyperplasic dermal regions are regions of new lymphatic vessel growth (termed lymphangiogenesis) or are normally present, dermal lymphatics that have “backfilled” with ICG-laden lymph.

Tortuous lymphatic vessels (Fig. 4[a], bottom). Tortuous main conducting vessels, as well as capillary lymphatic vessels, were seen in lymphedema subjects, but only rarely in normal subjects. Lymph transport in these lymphatic vessels appeared to deviate from the normal distal-to-proximal direction [17,18]. These vessels were typically dilated, filled completely with ICG, and did not “pump” ICG-laden lymph between lymphangions as actively as normal lymphatic vascular bundles.

Extravascular ICG (Figs. 4[b] and 4[c]). ICG was not associated with any apparent vessel, suggestive of lack of uptake by the initial lymphatic capillaries and extravascular transport. In some cases, ICG was even seen to diffuse distally from the site of injection towards the palm and fingers. Sometimes this extravascular ICG remained at or very near the site of ICG injection (nonmobile), and sometimes the ICG was found at a distance from the ICG injection site (mobile).

#167423 - $15.00 USD Received 3 March 2012; revised 27 Apr 2012; accepted 27 Apr 2012; published 3 May 2012

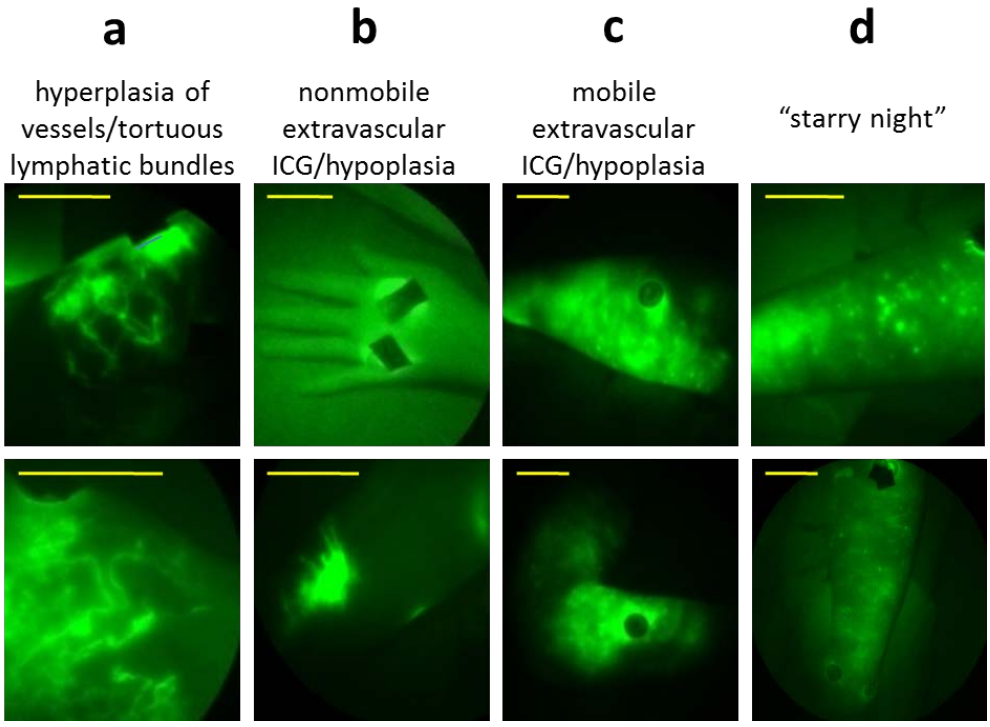

Fig. 4. Typical lymphatic architectural anomalies observed in BCRL subjects. (a) Hyperplasia/tortuous lymphatic vessels located on the medial elbow of a BCRL subject 13 years after onset (top) and the dorsal forearm of a subject 5 years after BCRL onset (bottom), (b) nonmobile extravascular ICG/hypoplasia on a dorsal hand of a subject 6 months after BCRL onset (top) and a dorsal forearm of a subject 6 months after BCRL onset (bottom), (c) mobile extravascular ICG/hypoplasia on the lateral forearm of a subject 6 months after BCRL onset (top) and on a medial elbow of a subject 6 months after BCRL onset (bottom), (d) punctuated ICG "clusters" located on the lateral forearm of a subject 5 years after BCRL onset (top) and on a lateral forearm of a subject 5 years after BCRL onset (bottom). Yellow scale bars = 5 cm.

Punctuated extravascular deposits of ICG (Fig. 4[d]). These previously reported architectural features [17–20] consist of "clusters" of extravascular ICG within the dermis. These clusters may arise due to backflow of ICG-laden lymph into the small initial lymphatics that normally drain the dermis. The association of ICG with lymph proteins may be responsible for the fluorescent "clusters" within the extravascular space. Adams *et al.* [19] reported the appearance of "starry-night" patterns after pneumatic compression treatment of an advanced BRCL subject, suggesting movement from the injection site to the dermis in a "backflow" condition not seen in normal subjects. The lymphatic vessel abnormalities visualized may develop in response to surgical, chemotherapeutical, or radiological damage, and may represent attempts to generate new lymphatic vessels, recruitment of normally underutilized vessels, or complete failure to use any vessels.

Figure 5 displays images from a group 3 representative, in which imaging was performed five years after lymphedema onset. Aberrations in the affected and contralateral, "unaffected" arm are notable, and include several types of anomalies, illustrating the heterogeneity of lymphatic abnormalities present.

#167423 - $15.00 USD Received 3 March 2012; revised 27 Apr 2012; accepted 27 Apr 2012; published 3 May 2012

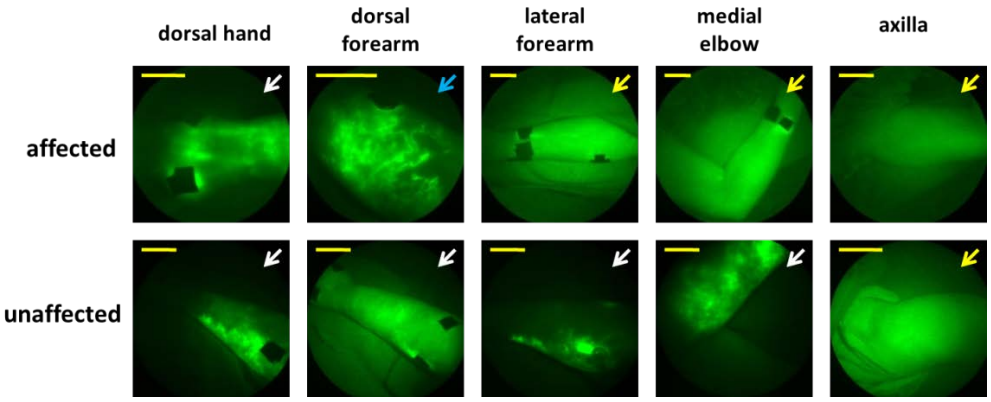

Fig. 5. Unaffected and affected (b) arms from one subject in group 3 (5 years since BCRL onset). Blue arrows = tortuous vessels/hyperplasia, yellow arrows = nonmobile extravascular ICG, white arrows = mobile extravascular ICG. Yellow scale bars = 5 cm.

3.3. Presence of lymphatic vessel architectural aberrations increases with time after onset of BCRL

Phenotypical abnormalities of lymphatics were assessed for each subject, and the abnormalities were tallied according to time since lymphedema onset. This retrospective analysis was designed to discover lymphatic phenotypes and was not powered to find differences between affected and unaffected arms of BCRL subjects as a function of time from initial onset of symptoms. Nonetheless, Fig. 6 shows the percentage of BCRL subjects in each group with onset of symptoms at (i) ≤6 months, (ii) between 6 months and 2 years, and (iii) greater than 5 years, exhibiting lymphatic abnormalities in affected and unaffected arms in the hands, ventral and dorsal forearms, elbows, and axilla.

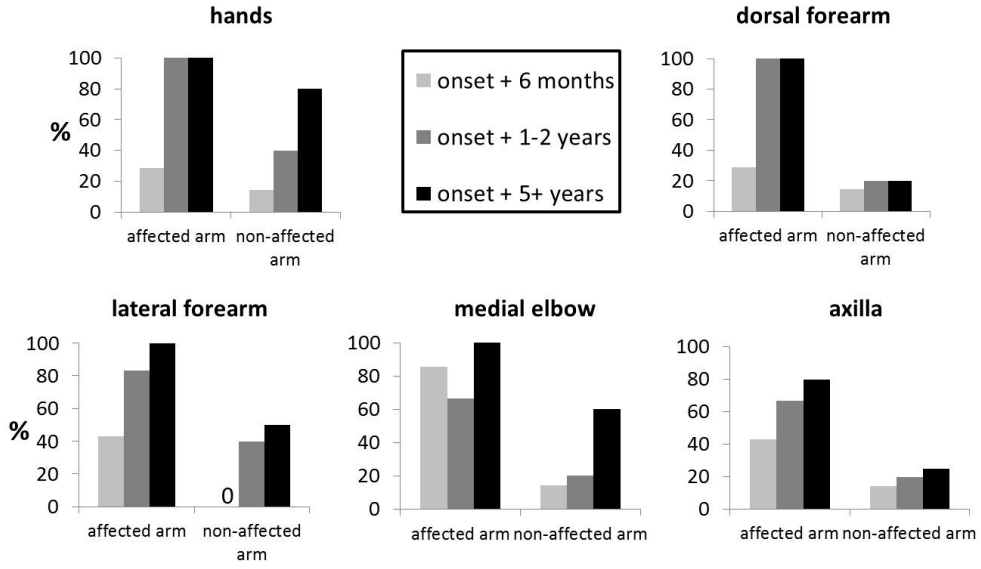

Fig. 6. Percent of images with architectural aberrations. Percent of (a) hands, (b) dorsal forearms, (c) ventral forearms, (d) medial elbows, and (e) axillary regions displaying lymphatic anomalies in groups 1 (6 months or less since onset), 2 (1-2 years since onset), and 3 (more than 5 years since onset).

#167423 - $15.00 USD Received 3 March 2012; revised 27 Apr 2012; accepted 27 Apr 2012; published 3 May 2012

Although the groups are too small and ill-defined to render the results conclusive, a trend toward increased lymphatic alterations with increased time from onset of symptoms is evident. Notably, both affected and "unaffected" arms display aberrations with increased time after BCRL onset.

4. Discussion

BCRL is currently diagnosed when arm volume increases beyond 20% of baseline measurements, or 20% of current contralateral, unaffected arm volume. Recent studies of breast cancer survivors at risk for BCRL found that earlier initiation of lymphedema management resulted in better outcome, and even complete resolution of BCRL [24,25]. Our study provided single "snapshots" of increased aberrant lymphatic architecture with time after self-reported onset of BCRL symptoms, and, remarkably, increased lymphatic anomalies in both afflicted and unafflicted arms were observed. If substantiated with longitudinal studies of individual subjects, these results have several clinical implications:

1. Current diagnosis of BCRL based upon differential afflicted and unafflicted arm volumes could result in underdiagnosis or late diagnosis, and could negatively impact the efficiencies of current manual therapies [24,25].
2. If systemic lymphatic dysfunction is a characteristic of BCRL, as this study suggests, then effective management should also include the contralateral arm and truncal lymphatic basins.

The technique of NIRF imaging used in this study is especially amenable to longitudinal studies, as it (i) requires no cannulation of lymphatic vessels, (ii) involves low dose (25 ug) and low volume (0.1 cc) administration of a dye that has a longstanding history of patient safety and rapid clearance (<2 minutes) through the hepatocirculatory system once it reaches the blood vasculature, and (iii) unlike emerging MRI (magnetic resonance) and CT (computed tomography) with lymphangiography agents [26,27], NIRF imaging distinguished the mixture of both functional and dysfunctional vessels observed in the early stages of BCRL, not just clearance rates of imaging agent. Because imaging is rapid (~200 milliseconds), involves a nonradioactive contrast agent, and provides both higher temporal and spatial resolution than conventional lymphoscintigraphy [21], repeated imaging can be routinely performed to evaluate change in lymphatic function with therapy.

The exact etiology of breast cancer-related lymphedema (BCRL) remains a mystery. The number of lymph nodes surgically removed has been reported to not affect cancer survival [28,29], although more extensive ALND and the addition of axillary radiation therapy increase risk of lymphedema [30,31]. A genetic predisposition for lymphatic dysfunction, other surgical or injury damage to lymphatics, body mass index, medications, and fitness level are all suspected systemic factors contributing to the development of lymphedema [32,33]. Using NIRF to capture a single snapshot of disease progression in a number of BCRL patients, we show the tendency not only for increased lymphatic abnormality, but potentially systemic involvement. Recently, in a study of unilateral lower extremity lymphedema patients, Burnand *et al.* used lymphoscintigraphy to monitor the percentage of 99mcTc that accumulated in the ilioinguinal regions 60 to 180 minutes after subcutaneous injection in the webspaces of the feet to show that clinically "normal" contralateral legs of patients with unilateral leg lymphedema also possessed lymphatic dysfunction [34]. Although their patient population was comprised of primary (hereditary and congenital) lymphedema subjects and their results showing bilateral disease might be expected, their results are nonetheless consistent with the trends observed in this study of BCRL. In two other studies of BCRL patients, rates of depot clearance after subcutaneous injection of radiolabeled protein in the hands and subsequent appearance in venous blood suggested lymphatic dysfunction in both affected and contralateral "normal" arms [35,36].

#167423 - $15.00 USD Received 3 March 2012; revised 27 Apr 2012; accepted 27 Apr 2012; published 3 May 2012

This retrospective study is subject to a number of disclaimers. Self-reported histories are subject to inaccuracy. Although H&Ps (health and physical reports written by an examining physician or other health care professional at time of consult) were used to compile background information, much of the information in these documents is subject-reported. Although subjects were asked to drink fluids before imaging sessions, hydration level variations were inevitable, possibly affecting results. Perhaps most importantly, study subjects received varying levels of lymphedema care and started therapy at different time points after onset, and these differences could affect outcomes [24,25]. Longitudinal imaging studies are needed to evaluate lymphatic remodeling that may occur prior to onset of BCRL symptoms, and further progress to include other body parts beyond the affected arm. Correlation of percent arm volume change with extent of lymphatic vessel architectural abnormalities could be documented in such prospective studies, similarly to published quantitative studies [37]. NIRF allow visualization of lymphatic vessels up to 4 centimeters deep. While other imaging modalities like photo-acoustic tomography (PAT) can image vascular structures at greater depths, PAT has no absorber in lymph for imaging. Finally, because NIRF is an investigational imaging technique, we were unable to combine with other confirmatory conventional imaging modalities, such as lymphoscintigraphy or rates of depot clearance of radiolabeled protein.

Lymphatic architectural abnormalities which varied widely in location were found in both the affected as well as unaffected, contralateral arms of subjects with BCRL, suggesting the disease may manifest itself systemically rather than locally. Since our retrospective evaluation demonstrated a trend of increased prevalence of lymphatic architectural abnormalities with increasing time since onset of symptoms, further studies need to determine whether systemic manifestation of lymphatic abnormalities in cancer-related lymphedema are indicative of progressive disease, or whether these abnormalities were present previously, but manifested in lymphatic overload only after cancer treatment.

5. Conclusions

This study illustrates the usefulness of NIRF imaging to track lymphatic aberration development in BCRL. The technology could also direct therapy, diagnosis, and even evaluate new radioprotective treatments [38]. The appearance of vessel abnormalities on unaffected arms with increasing time suggests that lymphedema has a systemic causal component, and that care should be given to both arms after cancer treatment. This study describes the apparent progression of BCRL by imaging lymphatic vasculature, and may provide key clues to causes, as well as providing impetus to encourage early, aggressive detection and treatment.

Acknowledgments

The authors would like to thank Kristin Adams, Chinmay Darne, Milton V. Marshall, I-Chih Tan, and XueJuan Wang for their contributions to this work, including subject imaging and clinical research coordination. This work was funded by National Institutes of Health U54 CA136404, R01 HL092923, and R01 CA12891.

#167423 - $15.00 USD Received 3 March 2012; revised 27 Apr 2012; accepted 27 Apr 2012; published 3 May 2012